Cell Metabolism
Article

Akt3 Deficiency in Macrophages Promotes Foam Cell Formation and Atherosclerosis in Mice

Liang Ding,[1] Sudipta Biswas,[1] Richard E. Morton,[2] Jonathan D. Smith,[2] Nissim Hay,[3] Tatiana V. Byzova,[1] Maria Febbraio,[1] and Eugene A. Podrez[1,*]
[1]Department of Molecular Cardiology
[2]Department of Cell Biology
Lerner Research Institute, Cleveland Clinic, Cleveland, OH 44195, USA
[3]Department of Biochemistry and Molecular Genetics, University of Illinois at Chicago, Chicago, IL 60607, USA
*Correspondence: podreze@ccf.org
DOI 10.1016/j.cmet.2012.04.020

SUMMARY

Akt, a serine-threonine protein kinase, exists as three isoforms. The Akt signaling pathway controls multiple cellular functions in the cardiovascular system, and the atheroprotective endothelial cell-dependent role of Akt1 has been recently demonstrated. The role of Akt3 isoform in cardiovascular pathophysiology is not known. We explored the role of Akt3 in atherosclerosis using mice with a genetic ablation of the *Akt3* gene. Using hyperlipidemic *ApoE*$^{-/-}$ mice, we demonstrated a macrophage-dependent, atheroprotective role for Akt3. In vitro experiments demonstrated differential subcellular localization of Akt1 and Akt3 in macrophages and showed that Akt3 specifically inhibits macrophage cholesteryl ester accumulation and foam cell formation, a critical early event in atherogenesis. Mechanistically, Akt3 suppresses foam cell formation by reducing lipoprotein uptake and promoting ACAT-1 degradation via the ubiquitin-proteasome pathway. These studies demonstrate the nonredundant atheroprotective role for Akt3 exerted via the previously unknown link between the Akt signaling pathway and cholesterol metabolism.

INTRODUCTION

Akt, also known as protein kinase B (PKB), plays an important role in the regulation of numerous cellular processes including cell growth, glucose metabolism, differentiation, proliferation, and apoptosis (Manning and Cantley, 2007). Three Akt isoforms, encoded by three separate genes, are expressed in mammals. The three isoforms are highly homologous in their amino acid sequences and display similar substrate specificity. Phenotypic analysis of the individual Akt isoforms' deletion in the mouse showed distinct phenotypes, which could be at least partially attributed to their relative expression in the affected tissues or organs. Combined deletions of the Akt isoforms in the mouse suggest compensatory and complementary roles of three isoforms (Manning and Cantley, 2007). However, the three isoforms may have distinct functions, even at the cellular level, even though the mechanisms of specificity are poorly understood. Despite recent discoveries, a thorough understanding of the specific roles of Akt family members and the molecular mechanisms that determine Akt isoform functional specificity is still lacking.

Akt is at the center of a complex signaling network regulating multiple cellular functions, suggesting a possibility that Akt signaling pathways may be involved in pathogenesis of atherosclerosis. However, studies of the role of Akt in general, and specifically Akt isoforms in atherogenesis, are very limited. Recent studies have shown that the genetic ablation of *Akt1* promotes coronary atherosclerosis (Fernandez-Hernando et al., 2007). The effect of Akt1 deficiency was mostly due to the enhanced expression of proinflammatory genes in the artery wall. Bone marrow transplantation experiments demonstrated that macrophages from *ApoE*$^{-/-}$*Akt1*$^{-/-}$ donors did not confer increased atherogenesis, suggesting that lesion expansion in the *ApoE*$^{-/-}$*Akt1*$^{-/-}$ mice might be of vascular origin. In agreement with these results, in vitro studies demonstrated that *Akt1*$^{-/-}$ macrophages tended to accumulate less cholesterol when exposed to modified lipoproteins. The roles of Akt2 and Akt3 isoforms, as well as specific involvement of Akt in lipid metabolism leading to modulation of atherosclerosis, are unknown.

In the present study, we explored the role of Akt3 in atherosclerosis using mice with a genetic ablation of the *Akt3* gene. We demonstrated a specific, macrophage-dependent, antiatherosclerotic role for Akt3 in hyperlipidemic *ApoE*$^{-/-}$ mice. Mechanistically, Akt3 exerts its atheroprotective function by restricting cholesteryl ester (CE) accumulation in macrophages via downregulation of lipoprotein uptake and inhibition of ACAT-1 protein expression. Thus, our study demonstrates a nonredundant atheroprotective role for Akt3 exerted via a link between Akt signaling pathway and lipoprotein and cholesterol metabolism.

RESULTS

Akt3 Deficiency Promotes Atherosclerosis in Hyperlipidemic *ApoE*$^{-/-}$ Mice

To study the functional role of Akt3 in atherogenesis in vivo, we subjected age- and sex-matched *ApoE*$^{-/-}$*Akt3*$^{-/-}$ and *ApoE*$^{-/-}$ mice to a Western diet for 9 weeks. En face analyses of total aorta

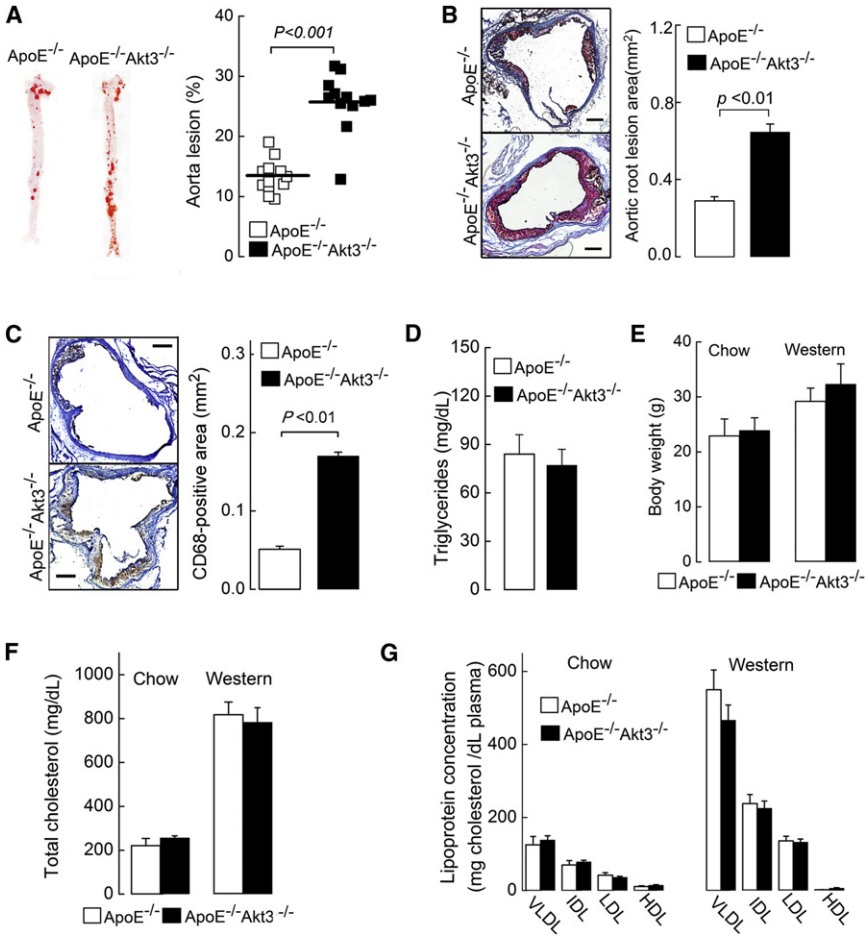

Figure 1. Deficiency of Akt3 Promotes Atherosclerosis in *ApoE*$^{-/-}$ Mice

(A) Representative images of en face oil red O staining of aortas of *ApoE*$^{-/-}$*Akt3*$^{-/-}$ and *ApoE*$^{-/-}$ littermates (eight males and four females in each group), n = 12.

(B) (Left panel) Representative images of cross-sections of the aortic sinus stained with oil red O. (Right panel) Quantification of atheroma area. Six slides form different layers were taken for analysis from at least three hearts for each group.

(C) (Left panel) CD68-positive macrophages (brown) in lesions of *ApoE*$^{-/-}$*Akt3*$^{-/-}$ and *ApoE*$^{-/-}$ mice. (Right panel) Quantification of CD68-positive areas.

(D) Fasting triglycerides levels of *ApoE*$^{-/-}$*Akt3*$^{-/-}$ and *ApoE*$^{-/-}$ mice after 9 weeks on a Western diet.

(E–G) Body weight, fasting cholesterol levels, and lipoprotein profiles from *ApoE*$^{-/-}$ and *ApoE*$^{-/-}$*Akt3*$^{-/-}$ mice on a normal chow diet or a Western diet. Data represent means ±SEM.

surfaces revealed an ~2-fold increase in the atherosclerotic lesion area in *ApoE*$^{-/-}$*Akt3*$^{-/-}$ mice (Figure 1A). Lesion areas in cross-sections of the aortic sinus were also increased 2.2-fold in *ApoE*$^{-/-}$*Akt3*$^{-/-}$ mice (Figure 1B). The areas infiltrated by CD68-positive macrophages in lesions were increased 3-fold in *ApoE*$^{-/-}$*Akt3*$^{-/-}$ mice (Figure 1C). The body weights, plasma cholesterol levels, plasma triglycerides (TGs), and lipoprotein profiles were similar between both genotypes fed a Western diet (Figures 1D–1G). Interestingly, plasma TGs were higher in *ApoE*$^{-/-}$*Akt3*$^{-/-}$ mice fed a chow diet (Figure S1). Thus, the genetic loss of *Akt3* increases aortic atherogenesis without changes in plasma cholesterol and lipoprotein profile. A similar result has been previously published for *Akt1*$^{-/-}$ mice (Fernandez-Hernando et al., 2007), indicating that Akt3 and Akt1 have nonredundant atheroprotective roles.

Akt3 Expression in Bone Marrow Cells Is Atheroprotective

To determine whether Akt3 deficiency in bone marrow contributes to atherogenesis, we created *ApoE*$^{-/-}$ chimeric mice with either *ApoE*$^{-/-}$*Akt3*$^{-/-}$ bone marrow or *ApoE*$^{-/-}$*Akt3*$^{+/+}$ bone marrow cells. After 10 weeks on a Western diet, the area of atherosclerotic lesions in the aorta was significantly increased in the *ApoE*$^{-/-}$*Akt3*$^{-/-}$ chimeras (41% increase, Figure 2A), while body weight, plasma cholesterol, and TGs were undistinguishable in two groups (Figures 2B–2D). Enhanced lesion areas in the aortic sinus were also observed in this group (Figure 2E). The aortic lesions in both groups consisted mainly of CD68-positive macrophage foam cells (Figure 2F). These findings strongly suggest that the Akt3 expression in macrophages is atheroprotective. Moreover, a similar extent of increase in atherosclerosis in bone marrow chimeras and in whole-body *Akt3* knockouts suggests that loss of Akt3 expression in bone marrow (presumably in macrophages) drives an increase in atherosclerosis development in Akt3 deficiency. Thus, the mechanism of atheroprotective function of Akt3 is different from that of Akt1.

Akt3 Deficiency Does Not Affect Macrophage Survival

Macrophage apoptosis is an important event in atherosclerosis plaque development (Tabas, 2010). We compared apoptosis of macrophages in atherosclerotic lesions of *ApoE*$^{-/-}$ and *ApoE*$^{-/-}$*Akt3*$^{-/-}$ mice. There was no increase in the percentage of TUNEL-positive CD68-positive macrophages (Figure 2G). We also tested in vitro whether *Akt3*$^{-/-}$ thioglycollate-elicited murine peritoneal macrophages (MPMs) are prone to apoptosis by culturing MPMs in the presence of acLDL and ACAT inhibitor FR-179254. This condition induces accumulation of unesterified cholesterol and, consequently, apoptosis in MPMs. While FR-179254 induced significant increase in apoptosis and a reduction in viability of MPMs, we saw no statistically significant difference between wild-type (WT) and *Akt3*$^{-/-}$ MPM, neither in the absence nor in the presence of FR-179254 (Figures 2H and 2I). These data indicate that macrophage Akt3 deficiency plays no significant role in apoptosis of macrophages, and that proatherosclerotic phenotype of *Akt3*$^{-/-}$ macrophages is apoptosis independent.

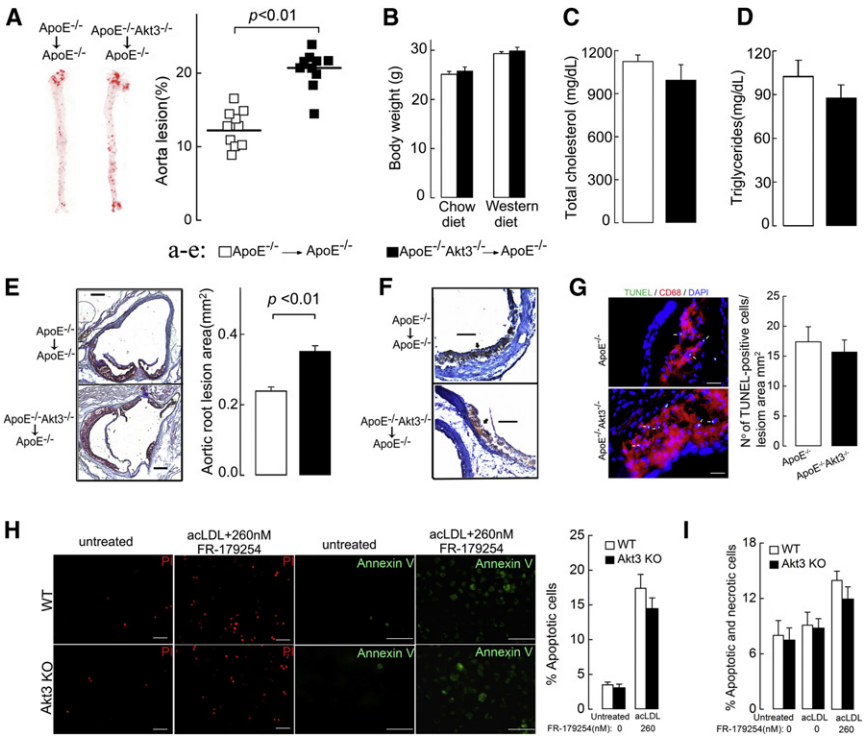

Figure 2. Atherosclerotic Lesion Development Is Increased in *ApoE*$^{-/-}$ Chimeras with *ApoE*$^{-/-}$*Akt3*$^{-/-}$ Bone Marrow

(A) Lesion analyses of aortas from *ApoE*$^{-/-}$ chimeras with *ApoE*$^{-/-}$*Akt3*$^{-/-}$ or *ApoE*$^{-/-}$ bone marrow, n = 10.

(B) Body weight of *ApoE*$^{-/-}$ chimeras before and after 10 weeks on a Western diet.

(C and D) Fasting cholesterol and triglycerides levels of *ApoE*$^{-/-}$ chimeras after 10 weeks on a Western diet, n = 7.

(E) Representative examples of cross-sections from the aortic sinus stained with oil red O and quantification of atheroma area, n = 7.

(F) CD68-positive macrophages (brown) in lesions of *ApoE*$^{-/-}$*Akt3*$^{-/-}$ and *ApoE*$^{-/-}$ mice. Scale bar, 100 μm; n = 7.

(G) Apoptotic cells and macrophages in lesions of *ApoE*$^{-/-}$ and *ApoE*$^{-/-}$*Akt3*$^{-/-}$ mice after 9 weeks of a Western diet as detected by TUNEL and CD68 staining, respectively. Scale bar, 25 μm; n = 7.

(H and I) Wild-type (WT) and *Akt3*$^{-/-}$ macrophages were treated with acLDL (100 μg/ml) in the presence or absence of ACAT inhibitor FR-179254, and (H) apoptosis was detected 48 hr after treatment using Annexin V-FITC or propidium iodide (PI) staining. Right panel shows quantification of the data for PI staining. Scale bar, 50 μm; n = 8. (I) Cell viability was determined by trypan blue exclusion 24 hr after treatment. n = 8. Data represent means ±SEM.

Deletion of *Akt3* Promotes Macrophage Cholesterol Accumulation and Foam Cell Formation In Vitro

Accumulation of cholesterol and CEs in macrophages and subsequent foam cell formation is a critical early step in atherogenesis. We tested whether the deletion of *Akt3* affects macrophage cholesterol accumulation and foam cell formation in vitro. The expression of Akt3 in WT MPM and the absence of Akt3 protein in MPMs of *Akt3*$^{-/-}$ mice were confirmed using an Akt3-specific antibody (see Figure S2A online). Western blot analysis of *Akt3*$^{-/-}$ MPMs using pan-Akt antibody revealed that total Akt levels decreased in *Akt3*$^{-/-}$ MPMs by ~25% (Figure 3A). Total Akt kinase activity was reduced by ~20% in *Akt3*$^{-/-}$ MPMs (Figure 3B). *Akt3*$^{-/-}$ and WT MPMs were cultured in the presence of either native LDL (negative control), acLDL, or serum from hyperlipidemic *ApoE*$^{-/-}$ mice known to contain atherogenic lipoprotein. We also used LDL modified by mild oxidation by the MPO-H_2O_2-NO_2^- system, or strong oxidation by Cu^{2+}. The initial cholesterol and CE content of *Akt3*$^{-/-}$ MPMs was indistinguishable from that of WT MPMs (Figure 3C). However, after 24 hr of exposure to modified LDL, *Akt3*$^{-/-}$ MPMs accumulated significantly more CE than did WT MPMs (Figures 3C and 3D; data for acLDL and hyperlipidemic serum are shown). Increase in unesterified cholesterol content was less pronounced. Neither MPM accumulated a significant amount of cholesterol upon incubation with native LDL as anticipated (data not shown). Neutral lipid staining with oil red O also revealed a noticeable increase in foam cell formation in *Akt3*$^{-/-}$ MPMs exposed to either acLDL or serum from hyperlipidemic *ApoE*$^{-/-}$ mice as compared to WT MPMs (Figure S2B). This effect was specific for Akt3, since *Akt1*$^{-/-}$ MPMs displayed reduced foam cell formation as compared to WT MPM (Figure S2C), in agreement with published data (Fernandez-Hernando et al., 2007). We also assessed CE formation by measuring the incorporation of [^{14}C]oleate into the CE of MPMs. Taking into account that variations in cholesterol efflux can contribute to cholesterol accumulation in MPMs, we exposed *Akt3*$^{-/-}$ and WT MPMs to increasing concentrations of acLDL in the media containing either no specific cholesterol acceptors (bovine serum albumin, BSA), only nonlipoprotein cholesterol acceptors (lipoprotein-deficient serum, LPDS), or complete spectrum of cholesterol acceptors (fetal bovine serum, FBS) (Figure 3E). We observed dose-dependent increases in CE formation in both *Akt3*$^{-/-}$ and WT MPMs; however, the increase was more pronounced in *Akt3*$^{-/-}$ MPMs in all conditions used. Thus Akt3 deficiency in MPM is associated with increased accumulation of CE and increased macrophage foam cell formation in vitro.

Akt3$^{-/-}$ MPMs Display Mild Increase in Uptake of Modified LDL and No Significant Change in De Novo Cholesterol Synthesis

To investigate whether the enhanced CE accumulation and foam cell formation in *Akt3*$^{-/-}$ macrophages was due to an increased uptake of modified forms of LDL, we first assessed the expression of major scavenger receptors (CD36, SR-AI, and LOX-1) in *Akt3*$^{-/-}$ and WT MPMs. No significant difference between the two groups was observed (Figure 4A). Since modified LDL can modulate the expression of scavenger receptors on macrophages (Han and Nicholson, 1998), we compared the expression of scavenger receptors on MPMs exposed to modified LDL.

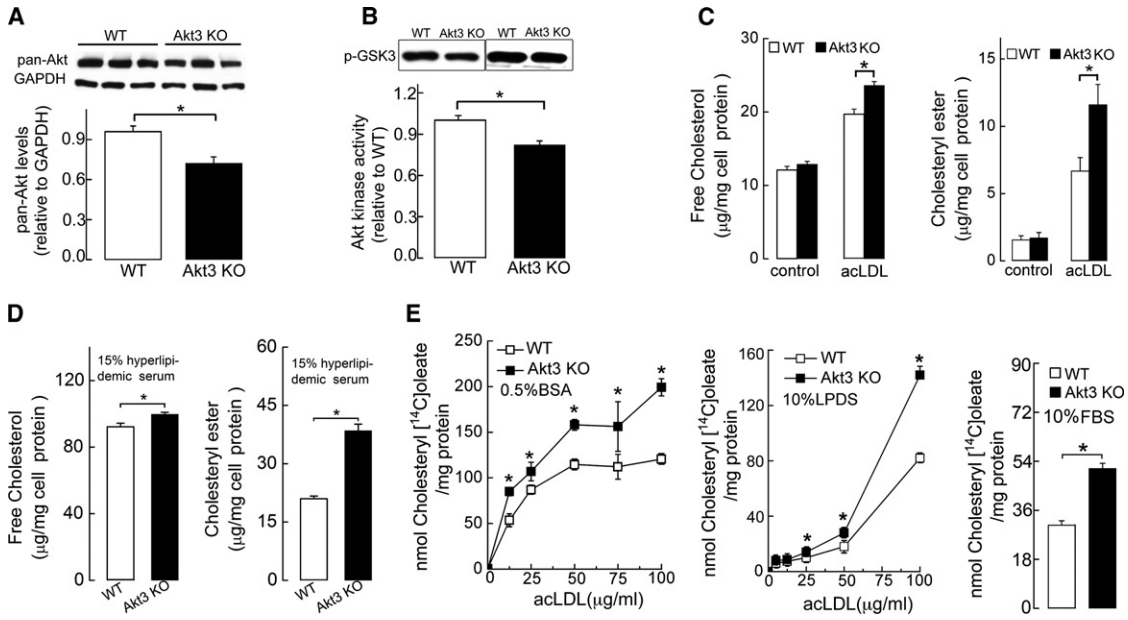

Figure 3. Deficiency of Akt3 in Murine Peritoneal Macrophages Promotes Cholesterol Ester Accumulation

(A) Western blot analyses of total Akt expression (using pan-Akt antibodies) in MPMs of wild-type (WT) and *Akt3*$^{-/-}$ (Akt3 KO) mice. n = 5.

(B) In vitro Akt kinase assay of MPM from WT and *Akt3*$^{-/-}$ mice. n = 5.

(C and D) The content of unesterified cholesterol and CE in WT and *Akt3*$^{-/-}$ MPMs before or after 24 hr incubation in (C) RPMI/10% LPDS medium containing 50 μg/ml acLDL or (D) RPMI containing 15% serum from hyperlipidemic *ApoE*$^{-/-}$ mice. n = 5.

(E) Cholesterol [^{14}C]oleate synthesis in WT and *Akt3*$^{-/-}$ MPMs incubated for 24 hr with indicated concentrations of acLDL and 1.5 μCi/ml [^{14}C]oleic acid in RPMI containing either BSA, LPDS, or FBS. n = 5. Data represent means ±SEM. *p < 0.05.

Again, no significant differences between the two groups were observed (Figures 4B and Figure S3A). Furthermore, binding assay at 4°C using modified LDL ligands for scavenger receptors revealed no significant difference between *Akt3*$^{-/-}$ and WT MPMs (Figure 4C), demonstrating that Akt3 deficiency does not induce expression of scavenger receptors. Since alternative pathways have been described to mediate the uptake of modified LDL, such as macro- and micropinocytosis, phagocytosis, and contribution of other receptors, we assessed uptake of modified LDL at 37°C. We observed moderate and uniform increases in uptake of all forms of modified LDL tested by *Akt3*$^{-/-}$ MPM (Figure 4D). Since scavenger receptor expression was similar, these increases are probably explained by a small increase in pinocytosis that we observed in *Akt3*$^{-/-}$ MPM (Figure 4E). Even though these increases are small, theoretically they still may contribute to accumulation of cholesterol in *Akt3*$^{-/-}$ MPM.

Akt signaling pathways were recently implicated in the regulation of cholesterol synthesis. Theoretically, de novo cholesterol synthesis can contribute to the accumulation of cholesterol in macrophages. However, we found no significant difference in cholesterol synthesis between *Akt3*$^{-/-}$ and WT MPM in conditions that stimulate cholesterol synthesis (in the presence of LPDS), nor in conditions of increased cholesterol uptake and suppressed cholesterol synthesis (in the presence of modified LDL) (Figure 4F). These results suggest that Akt3 isoform is not involved in the regulation of cholesterol synthesis in macrophages, and, consequently, increased cholesterol synthesis does not contribute to the observed accumulation of CE in *Akt3*$^{-/-}$ macrophages.

Cholesterol Ester Hydrolysis Is Not Changed in *Akt3*$^{-/-}$ MPMs

Since we found only a modest 10%–15% increase in lipoprotein cholesterol uptake (Figure 4D) and no significant changes in cholesterol synthesis in *Akt3*$^{-/-}$ macrophages (Figure 4F), the only way to significantly increase CE content in MPM is via a reduction of efflux of lipoprotein-derived cholesterol. The question remains, is this decrease due to a primary effect on the efflux machinery, or secondary, due to (1) the defect in lysosomal hydrolysis of lipoprotein-derived CE, (2) an increased esterification of cholesterol by ACAT, or (3) a reduced hydrolysis of ACAT-derived CE by neutral CE hydrolases. To test the possibility that a defect in the hydrolysis of LDL-derived CE exists in *Akt3*$^{-/-}$ MPMs, we incubated MPMs with acLDL in the presence of the ACAT inhibitor FR179254. Inhibition of CE synthesis by FR179254 in WT and *Akt3*$^{-/-}$ MPMs was associated with complete suppression of neutral lipid accumulation, demonstrating that the accumulation of CE in *Akt3*$^{-/-}$ MPMs is ACAT dependent (Figure S3B). The possibility of changes in hydrolysis of endogenously formed CE in *Akt3*$^{-/-}$ MPMs was then investigated. LIPE, or hormone sensitive lipase, and nCEH1 account for nearly 90% of CE hydrolysis in macrophages (Sekiya et al., 2009). The expression of both enzymes in WT and *Akt3*$^{-/-}$ macrophages was similar (Figure 4G). We also assessed the rate of CE hydrolysis in CE-laden cultured MPMs, and found that the rates were almost identical in WT and *Akt3*$^{-/-}$ macrophages (Figure 4H). Together, these data indicate that Akt3 deficiency does not suppress CE hydrolysis in MPM.

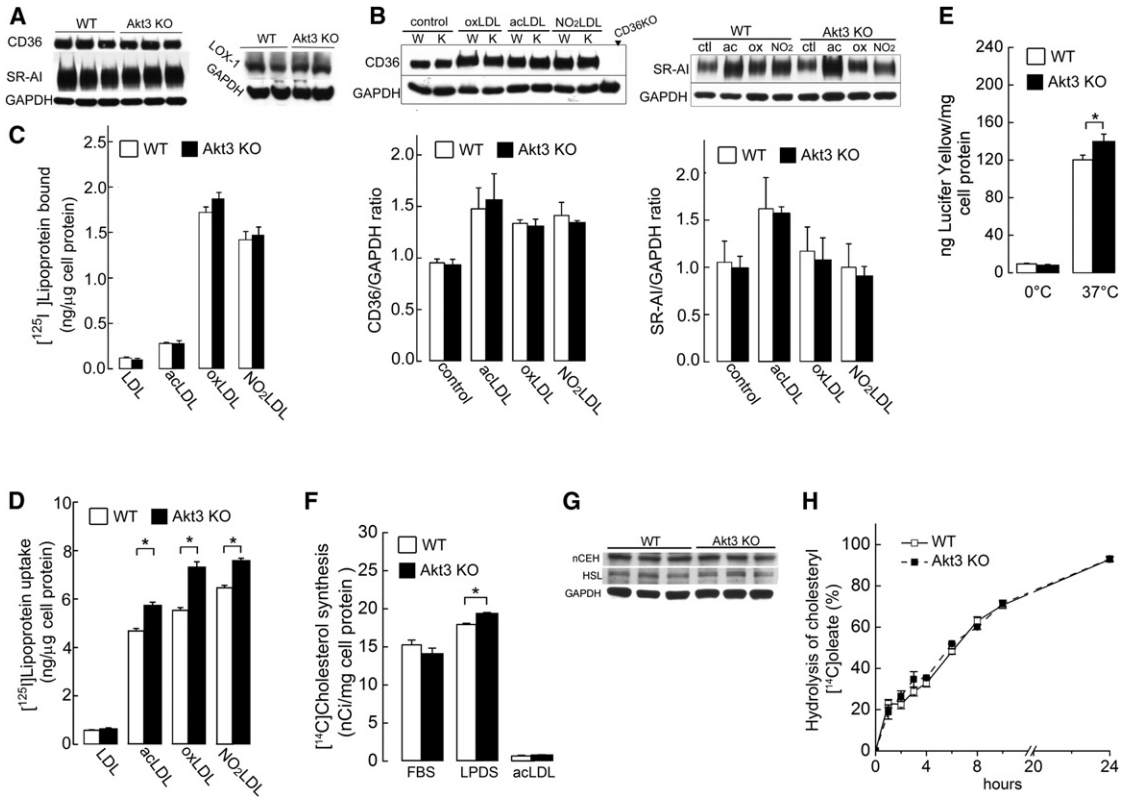

Figure 4. Deletion of *Akt3* Does Not Significantly Change Macrophage Expression of Main Scavenger Receptors, Main Cholesteryl Ester Hydrolases, Cholesterol Synthesis, and Hydrolysis of Cholesterol Esters and Results in Mild Increase in Uptake of Modified LDL

(A) Western blot analyses of scavenger receptor (CD36, SR-AI, LOX-1) expression on MPMs of WT and *Akt3*$^{-/-}$ mice. n = 6.

(B) Expression of CD36 and SR-AI on MPM after 18 hr incubation with or without 50 μg/ml of modified LDL. Graph below shows densitometric quantification. MPMs from *CD36*$^{-/-}$ mice were used as a negative control of CD36 expression. n = 6.

(C) MPMs from WT and *Akt3*$^{-/-}$ mice were incubated for 2 hr on ice with 10 μg/ml of ^{125}I-labeled native or modified LDL, and total bound ^{125}I was quantified. n = 5.

(D) MPMs from WT and *Akt3*$^{-/-}$ mice were incubated for 6 hr 37°C with 10 μg/ml of ^{125}I-labeled native or modified LDL, and total uptake of ^{125}I-lipoprotein was quantified. n = 6.

(E) Uptake of the lucifer yellow fluid-phase dye as a measure of pinocytosis in WT and *Akt3*$^{-/-}$ MPMs. n = 6.

(F) [^{14}C]Cholesterol synthesis determined by the incorporation of [^{14}C] acetyl CoA in [^{14}C]cholesterol in WT and *Akt3*$^{-/-}$ MPMs cultured in RPMI/10% FBS, RPMI/10% LPDS or RPMI/10% LPDS + 50 μg/ml acLDL (for details, see the Supplemental Information). n = 6.

(G) Western blot analyses of CE hydrolase (nCEH, HSL) expression in MPMs of WT and *Akt3*$^{-/-}$ mice. n = 5.

(H) Hydrolysis of cholesteryl [^{14}C]oleate in WT and *Akt3*$^{-/-}$ MPMs in the presence of ACAT inhibitor (for details, see the Supplemental Information). n = 5. Data represent means ±SEM. *p < 0.05.

Expression and Activity of ACAT-1 Are Increased in *Akt3*$^{-/-}$ MPMs

Excess free cholesterol in macrophages undergoes esterification by acyl-CoA:cholesterol acyltransferase (SOAT or ACAT). Two isoforms of ACAT (ACAT-1 and ACAT-2) are found in mammalian cells (Li and Glass, 2002). We assessed both protein expression and enzyme activity of ACAT-1 and ACAT-2 in *Akt3*$^{-/-}$ and WT MPM. Akt3 deficiency led to elevated expression of ACAT-1 protein (~35% increase), while no noticeable change in ACAT-2 protein expression was detected (Figures 5A and 5B). Expression of ACAT-1 in *Akt3*$^{-/-}$ MPMs was upregulated upon incubation with acLDL and was 2.5-fold higher compared to WT MPMs (Figure 5C). In contrast, changes in ACAT-2 expression in response to incubation with acLDL were modest (Figure 5D). Akt3 deficiency in MPM was associated with a 1.9-fold increase in ACAT enzymatic activity (Figure 5E). Cholesterol loading after incubation with acLDL led to further increases in ACAT activity in both WT and *Akt3*$^{-/-}$ MPMs; however, ACAT activity was still 2-fold higher in *Akt3*$^{-/-}$ MPM.

While western blot analysis revealed an increased expression of both ACAT-1 and ACAT-2 after exposure to acLDL, ACAT-2 is considered to play no significant role in the accumulation of CE in macrophages (Rudel et al., 2001). We performed foam cell formation and CE synthesis assays in the presence of a selective ACAT-2 inhibitor, pyripyropene A (PPPA) (Das et al., 2008), and confirmed that ACAT-1 is the major isoform of ACAT responsible for cholesterol accumulation in *Akt3*$^{-/-}$ MPMs (Figures S4A–S4C). These data suggest that increased ACAT-1 expression and activity may play a significant role in excessive CE accumulation in *Akt3*$^{-/-}$ MPMs.

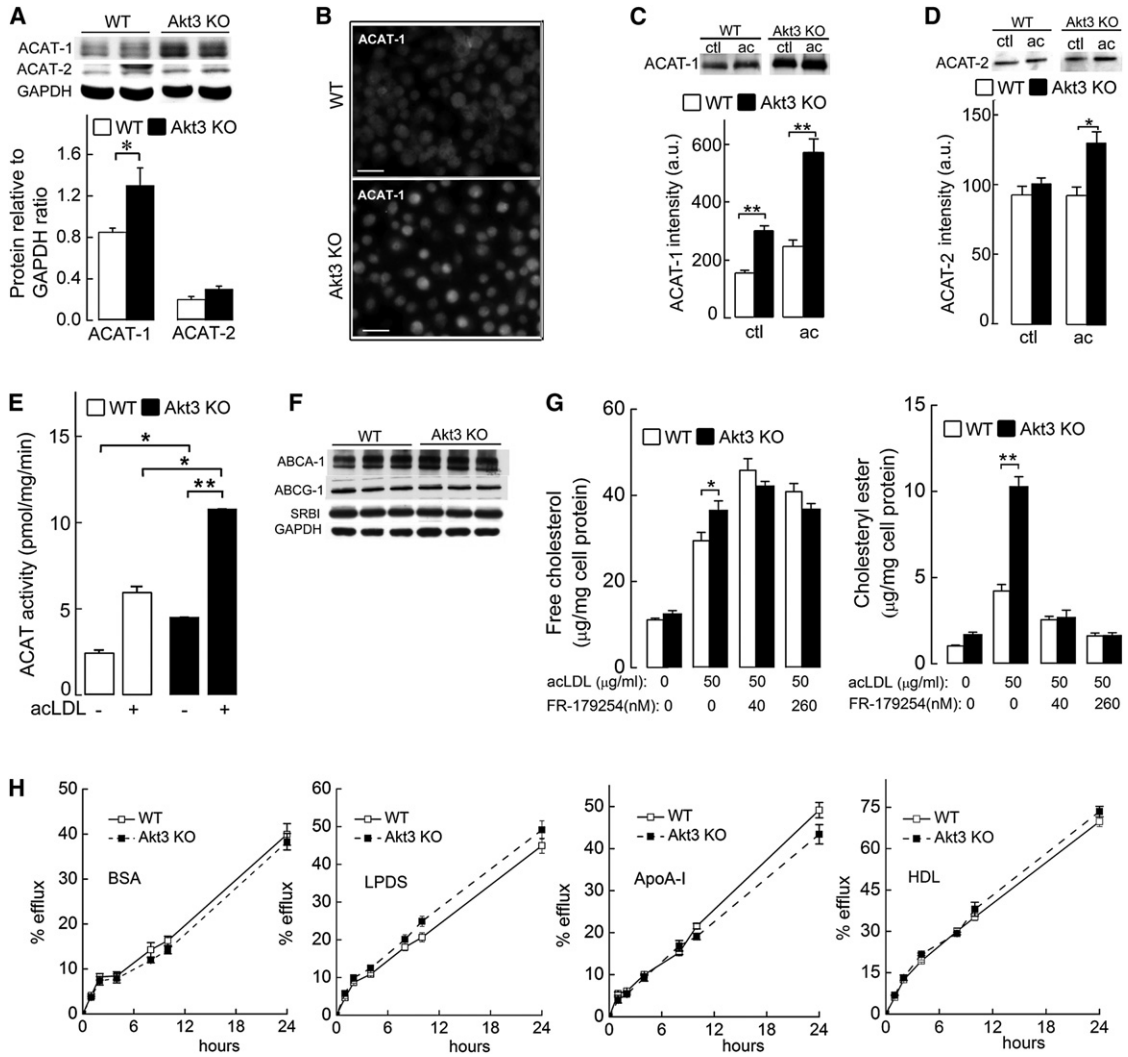

Figure 5. *Akt3*$^{-/-}$ Macrophages Have Increased Expression and Activity of Acyl-CoA:Cholesterol Acyltransferase and Have No Significant Changes in Cholesterol Efflux

(A) Western blot analyses of ACAT-1 and ACAT-2 expression in WT and *Akt3*$^{-/-}$ MPMs. n = 4.

(B) Immunofluorescence staining of ACAT-1 in WT and *Akt3*$^{-/-}$ MPMs. Scale bar, 100 μm.

(C and D) Immunoprecipitation and subsequent western blot analysis and densitometric quantification of ACAT-1 and ACAT-2 in MPMs of WT or *Akt3*$^{-/-}$ mice after 18 hr incubation with or without (ctl) 50 μg/ml of acLDL. n = 6.

(E) In vitro ACAT activity in lysates of WT and *Akt3*$^{-/-}$ MPMs after 18 hr -incubation with or without 50 μg/ml of acLDL. n = 6.

(F) Western blot analysis of ABCA-1, ABCG-1, and SR-BI expression in WT and *Akt3*$^{-/-}$ MPM. n = 3.

(G) The content of unesterified and esterified cholesterol in WT and *Akt3*$^{-/-}$ MPMs incubated with 50 μg/ml acLDL in the presence of indicated concentrations of ACAT inhibitor FR179254. n = 5.

(H) MPMs from WT or *Akt3*$^{-/-}$ mice were incubated overnight with 100 μg/ml of acLDL and 3 μCi/ml ^{3}H-cholesterol, washed, and equilibrated, and then cholesterol efflux was assessed into the media containing either 0.5% BSA, 5% LPDS, 50 μg/ml ApoA-I, or 100 μg/ml HDL in the presence of 80 nM FR179254 over a 24 hr period. n = 6. Data represent means ±SEM. *p < 0.05; **p < 0.01.

Akt3$^{-/-}$ MPMs Have No Primary Defect in Cholesterol Efflux

We next tested whether *Akt3*$^{-/-}$ MPMs have a primary defect in cholesterol efflux. Lack of Akt3 expression has no noticeable effect on the expression of major mediators of cholesterol efflux ABCA1, ABCG1, or SR-BI on MPMs (Figure 5F). Initial experiments using ^{3}H-cholesterol tracer showed modestly reduced (5%–15% reduction) cholesterol efflux in *Akt3*$^{-/-}$ MPMs (Figure S4D). Since increased activity of ACAT-1 in *Akt3*$^{-/-}$ MPMs can reduce the pool of ^{3}H-cholesterol available for efflux, we next repeated cholesterol efflux experiments and performed direct measurements of cellular cholesterol mass in the presence of ACAT-1 inhibitor (Figures 5G and 5H). Cholesterol efflux from WT and *Akt3*$^{-/-}$ MPMs under these conditions was practically identical (Figure 5H). Inhibition of cholesterol esterification in MPMs exposed to modified LDL resulted in an increase in unesterified cholesterol mass, both in WT and *Akt3*$^{-/-}$ macrophages, as expected (Figure 5G). However, in agreement

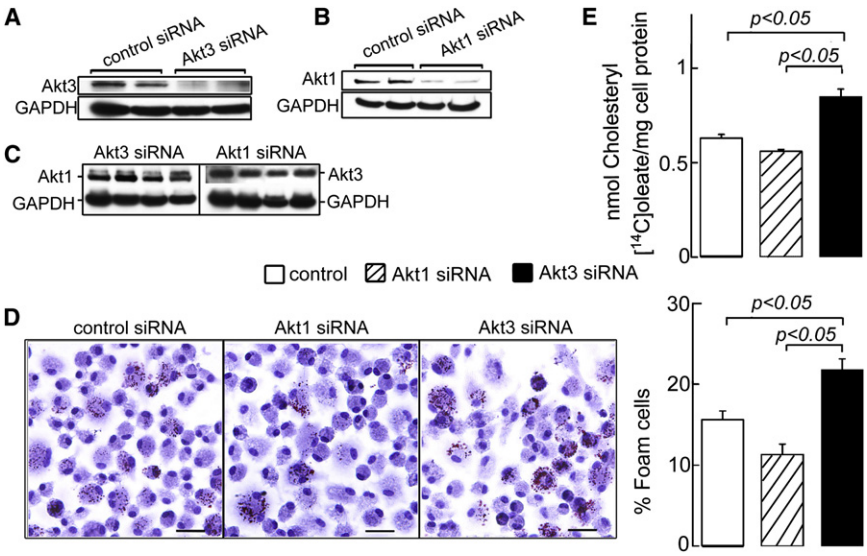

Figure 6. Inhibition of Akt3, but Not Akt1, by siRNA Promotes Foam Cell Formation in MPMs

(A–C) MPMs were transfected with either control siRNA or Akt1-specific or Akt3-specific siRNAs for 48 hr. Western blot was performed using anti-Akt1-, Akt3-, or GAPDH-specific antibodies.

(D) Foam cell formation in siRNA-treated MPMs. MPMs were transfected with siRNA for 72 hr and further incubated with 50 μg/ml acLDL in RPMI/0.5% BSA for 18 hr, then fixed and stained with oil red O. Right panel shows quantification of foam cells. Scale bar, 25 μm.

(E) MPMs were transfected as in (D) and incubated with 50 μg/ml of acLDL and 0.3 μCi/ml [^{14}C]oleic acid for 24 hr, and cholesterol [^{14}C]oleate synthesis was assessed. n = 5. Data represent means ±SEM.

with the results of the experiment on cholesterol efflux, there was no difference in cholesterol content between WT and *Akt3*$^{-/-}$ macrophages under these conditions. These experiments rule out a primary defect in cholesterol efflux from *Akt3*$^{-/-}$ MPMs as a mechanism leading to increased CE accumulation in *Akt3*$^{-/-}$ MPMs. They further suggest that a net decrease in cholesterol efflux of lipoprotein-derived cholesterol is secondary to enhanced cholesterol esterification mediated by ACAT-1.

Downregulation of Macrophage Akt3 Expression Augments CE Synthesis and Foam Cell Formation In Vitro

To test whether suppression of the expression of Akt3 in MPMs in vitro is sufficient to induce ACAT-1 expression and CE accumulation, we used the small interfering RNA to inhibit Akt3 expression in WT MPMs, and then performed foam cell formation and CE synthesis assays. As additional control, we used the same approach to suppress the expression of Akt1 in WT MPMs. Transfection with Akt3 siRNA significantly inhibited the expression of Akt3 without having an effect on Akt1 expression (Figures 6A and 6C and Figure S5A). In turn, Akt1 siRNA specifically inhibited Akt1 expression (Figure 6B and Figure S5A). Transfection efficiency in these experiments assessed using FITC-conjugated control siRNA reached 55% (Figure S5B). There were no significant changes in the subcellular distribution of Akt1 and Akt3 after treatment with specific siRNAs (Figure S5A). Inhibition of Akt3 expression resulted in increase in macrophage foam cell formation and in cholesteryl [^{14}C]oleate synthesis (Figures 6D and 6E). In contrast, inhibition of Akt1 expression tended to reduce foam cell formation and CE synthesis in MPMs. These results further support the direct and specific role of Akt3 in the excessive cholesterol accumulation in MPMs.

Akt1 and Akt3 Have Different Subcellular Distribution in Macrophages

To find out why Akt1 and Akt3 deficiencies lead to opposite effects on macrophage CE accumulation, we examined the subcellular distribution of Akt1 and Akt3 in macrophages. Immunofluorescent staining showed distinct localizations of Akt1 and Akt3 in WT MPMs. Akt1 was mainly located in the nucleus, while the majority of Akt3 was located in the cytoplasm (Figure 7A and Figure S6A). The deletion of *Akt3* led to no obvious change in Akt1 distribution in MPMs, suggesting that Akt1 cannot compensate for the lack of Akt3 expression (Figure 7B). The localization of Akt1 and Akt3 in human differentiated THP-1 macrophages was similar to that in MPMs (Figure 7C). This distribution of Akt3 and Akt1 was cell type specific since in hepatocytes (HepG2 cells) Akt3 had exclusively nuclear localization, while significant amount of Akt1 was observed in the cytoplasm (Figure S6B). Thus a moderate decrease in total Akt expression and activity in *Akt3*$^{-/-}$ macrophages can be associated with major lack of Akt activity and major effect on Akt targets in the cytoplasm of these cells.

Akt3 Regulates ACAT-1 Expression by Promoting Its Degradation via the Ubiquitin-Proteasome Pathway

To determine whether the increase in ACAT-1 expression was a consequence of an increase in *ACAT-1* transcript, we assessed *ACAT-1* mRNA level in WT, and *Akt3*$^{-/-}$ MPMs by RT-PCR and real-time RT-PCR. We observed no significant difference between these two groups (Figure 7D). Furthermore, no increase in the synthesis of ACAT-1 protein was found in *Akt3*$^{-/-}$ MPMs (Figure 7E). The elevation in ACAT-1 could be due to an increase in protein stability. We assessed the half-life of ACAT-1 protein in WT and *Akt3*$^{-/-}$ MPMs using cycloheximide to inhibit protein synthesis. As shown in Figure 7F, the half-life of ACAT-1 in WT MPMs was 8 hr, while in *Akt3*$^{-/-}$ MPMs the half-life of ACAT-1 increased to 18 hr. We next tested whether two primary intracellular protein degradation pathways, the ubiquitin-proteasome and lysosome pathways, are involved in accelerated degradation of ACAT-1 in WT macrophages. Treatment of WT MPMs, but not of *Akt3*$^{-/-}$ with specific proteasome inhibitor, MG132, resulted in a pronounced increase in ACAT-1 protein expression (Figure 7G). Chloroquine had no significant effect on ACAT-1 expression. The majority of cellular proteins

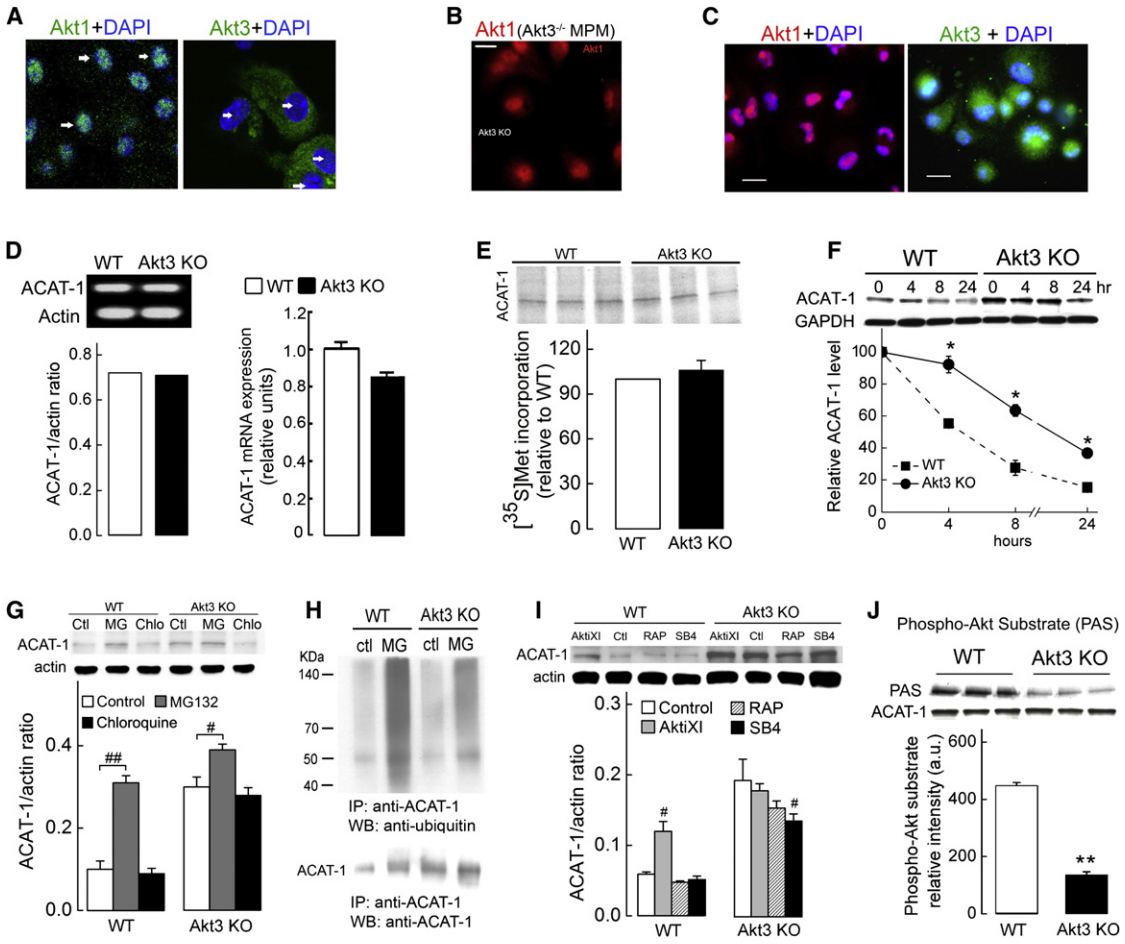

Figure 7. The Mechanism of Specific Regulation of ACAT-1 by Akt3

(A) Subcellular localization of Akt1 and Akt3 detected by the confocal immunofluorescence microscopy differs in MPMs. DAPI staining (blue, white arrow) is the nuclear marker.

(B) Immunofluorescence showed no significant changes in Akt1 localization in *Akt3*$^{-/-}$ MPMs.

(C) Immunofluorescence analysis of Akt1 (red) and Akt3 (green) localization in human differentiated THP-1 macrophages. Scale bar, 25 μm.

(D) Analysis of ACAT-1 mRNA expression in WT and *Akt3*$^{-/-}$ MPMs using semiquantitative RT-PCR (left panel) and quantitative real-time RT-PCR (right panel), actin mRNA used as a loading control. n = 4.

(E) Immunoprecipitation of ACAT-1 from WT and *Akt3*$^{-/-}$ macrophages lysates after a 2 hr pulse label with [^{35}S]methionine. Equal amounts (500 μg) of protein from macrophage cell lysates were immunoprecipitated with ACAT-1 antibodies and separated by SDS-PAGE before autoradiography. n = 3.

(F) MPMs from WT and *Akt3*$^{-/-}$ mice were incubated with cycloheximide (10 μg/ml), and at the indicated time points, cells were harvested, lysed, and analyzed for ACAT-1 levels by western blotting. GAPDH levels were used as a loading control. n = 3.

(G) Wild-type and *Akt3*$^{-/-}$ MPMs were treated with proteasome inhibitor MG132 (MG, 20 μM) or lysosome inhibitor chloroquine (chlo, 30 μM) for 16 hr. ACAT-1 and corresponding β-actin (control) protein level were examined by western blot analysis. n = 3.

(H) Cultured WT and *Akt3*$^{-/-}$ MPMs were treated with MG132 (MG, 20 μM) for 16 hr and the cell lysates immunoprecipitated (IP) using anti-ACAT-1 antibody, followed by SDS-PAGE and immunoblotting using anti-ubiquitin antibody and anti-ACAT-1 antibody.

(I) WT and *Akt3*$^{-/-}$ MPMs were treated with 40 μM Akt inhibitor XI (AktiXI), 20 nM rapamycin (RAP), or 10 μM SB 415286 (SB4) for 18 hr. The expression of ACAT-1 and β-actin (control) was assessed by western blot analysis. Lower panel shows densitometric quantification. n = 3.

(J) ACAT-1 recognition by phospho-Akt substrate antibody. Total cell lysates of WT and *Akt3*$^{-/-}$ MPMs were prepared and immunoprecipitated using anti-ACAT-1 antibody. IP product was analyzed using ACAT-1 and phospho-Akt substrate antibody. n = 6. Data represent means ±SEM. *$p < 0.05$ and **$p < 0.01$ versus wild-type; $^{\#}p < 0.05$ and $^{\#\#}p < 0.01$ versus control.

targeted for proteasomal degradation are first polyubiquitinated. WT and *Akt3*$^{-/-}$ MPMs were treated with MG132 and lysed, and then ACAT-1 was immunoprecipitated and subjected to SDS-PAGE and western blotting analysis using anti-ubiquitin antibody. Inhibition of proteasome pathway in WT macrophages resulted in significant accumulation of high-molecular-mass polyubiquitinated protein smear (Figure 7H), suggesting that ACAT-1 is polyubiquitinated in macrophages and that the polyubiquitinated forms of ACAT-1 are rapidly removed through the proteasome pathway. Polyubiquitination of ACAT-1 isolated from *Akt3*$^{-/-}$ MPMs was significantly reduced as compared to WT MPM (Figure 7H). Taken together, these results suggest that Akt3 suppresses ACAT-1 expression by promoting ACAT-1 degradation via the ubiquitin-proteasome mechanism.

Akt is at the center of a complex signaling network and directly phosphorylates multiple intracellular targets. While the pharmacological inhibition of Akt in WT MPMs led to a significant increase in ACAT-1 expression, no effect of inhibition of such major signaling pathways downstream of Akt as glycogen synthase kinase-3β pathway, mTOR pathway, or NF-κB pathway was observed (Figure 7I and Figure S6C). Interestingly, ACAT-1 possesses consensus phosphorylation sites for Akt, and direct phosphorylation by Akt is known to promote degradation via a proteasome pathway. To investigate whether ACAT-1 phosphorylation correlates with Akt3 expression, we immunoprecipitated ACAT-1 from MPMs and performed a western blotting analysis using a phospho-(Ser/Thr)-Akt substrate antibody (Sano et al., 2007). ACAT-1 isolated from *Akt3*$^{-/-}$ MPMs exhibited significantly reduced staining by this antibody as compared to WT MPMs (Figure 7J). We have also observed that Akt3 and ACAT-1 can be coimmunoprecipitated from cell lysate, suggesting a direct interaction (Figure S6D). These results suggest an intriguing possibility that ACAT-1 is a direct target of Akt3.

DISCUSSION

The specific role of Akt3 isoform in vivo is poorly understood. To date, it has been shown that Akt3 plays a specific role in brain development and function, as well as in selected types of cancer (Davies et al., 2008; Easton et al., 2005; Nakatani et al., 1999; Stahl et al., 2004; Tokuda et al., 2011; Tschopp et al., 2005). In this study, we demonstrated that genetic ablation of *Akt3* leads to accelerated atherosclerosis in hyperlipidemic *ApoE*$^{-/-}$ mice. Bone marrow transplantation experiments demonstrated that the atheroprotective role of Akt3 depends on its expression in bone marrow-derived cells, presumably macrophages. In vitro experiments have shown that even though Akt3 in macrophages is a minor isoform, its deletion leads to excessive intracellular accumulation of CE and increased foam cell formation. Mechanistically, increased CE accumulation and foam cell formation in the absence of Akt3 were linked to an increase in lipoprotein uptake and an increase in ACAT-1 activity and protein level.

Macrophage foam cell formation is an early key step in atherosclerosis. Macrophage survival in an atherosclerotic lesion is known to play an atheroprotective role in advanced atherosclerotic lesions but a proatherosclerotic role in early lesions (Tabas, 2010). Akt is known to promote cell survival, and recent studies have shown that Akt1, a major Akt isoform in macrophages, regulates apoptosis and necrosis of these cells both in vitro and in vivo (Fernandez-Hernando et al., 2007). Our results, on the other hand, strongly suggest that macrophage Akt3 plays a minor role in macrophage survival, and that the proatherosclerotic phenotype of *Akt3*$^{-/-}$ macrophages is apoptosis independent. This finding is consistent with the previously reported lack of the effect of Akt3 deficiency on cell survival in other cell types (Wright et al., 2008).

Mechanisms of foam cell formation may include increased uptake of atherogenic lipoproteins, disturbed intracellular processing, and ineffective elimination of cholesterol from cells via the cholesterol efflux pathway. We have ruled out changes in cholesterol synthesis and cholesterol ester hydrolysis, and a primary defect in cholesterol efflux machinery as significant contributors to excessive CE accumulation in *Akt3*$^{-/-}$ MPMs. According to our data, at least two mechanisms contribute to this effect. We observed a small but consistent increase in modified lipoprotein uptake in *Akt3*$^{-/-}$ MPMs, even though the expression of three major scavenger receptors was not changed. Mechanistically, this increase is explained by the mild increase in pinocytosis that we found in *Akt3*$^{-/-}$ MPMs. It has been demonstrated that fluid-phase pinocytosis contributes to macrophage cholesterol accumulation within mouse atherosclerotic plaques (Kruth, 2011). Theoretically, a mild increase in lipoprotein uptake could lead to a significant increase in CE accumulation in macrophages over time, but only if unmatched by an equivalent increase in efflux. Our second observation can provide a mechanism for the reduction in cholesterol efflux in *Akt3*$^{-/-}$ MPMs. We observed that macrophage Akt3 deficiency specifically augments expression of ACAT-1, an enzyme diverting cholesterol from the cholesterol efflux pathway by esterifying cholesterol and promoting its storage in cytoplasmic droplets. ACAT-1 is the major isoenzyme in lipid-laden macrophages, both in vitro and in vivo. It is localized in endoplasmic reticulum (ER)-regulating cholesterol content in ER and plays a critical role in CE accumulation in cells in atherosclerotic lesions (Miyazaki et al., 1998).

The concept that increased accumulation of CE in macrophages is proatherogenic is supported by the demonstration of increased atherosclerosis in mice with knockout of the two major enzymes responsible for CE hydrolysis in macrophages (Sekiya et al., 2009), as well as by the finding that overexpression of cholesteryl-ester hydrolase in macrophages protects against diet-induced atherosclerosis (Zhao et al., 2007). Overexpression of ACAT-1 suffices to induce cholesterol ester accumulation in vitro (Liang et al., 2004). We confirmed this observation using RAW264.7 mouse macrophage cells. Complete suppression of CE formation in macrophages in vivo as in ACAT-1 deficiency leads to the formation of large macrophage-poor atherosclerotic lesions, because some ACAT-1 activity is required for the macrophage to survive in conditions of increased lipoprotein uptake, typical for proatherosclerotic environment (Chang et al., 2009). On the other hand, the concept that increased ACAT-1 expression in macrophages plays a proatherosclerotic role is supported by animal and in vitro studies (Ikenoya et al., 2007; Worthley et al., 2007). Our in vivo and in vitro data suggest that genetic manipulation leading to increased expression and activity of ACAT-1 in macrophages is proatherogenic. Thus, published data and our data suggest that both complete prevention of cholesterol esterification and augmented accumulation of CEs in macrophages promote atherosclerosis, but via different mechanisms.

ACAT-1 is regulated at both transcriptional and posttranslational levels. It is allosterically activated by the binding of cholesterol (Chang et al., 2009). Expression of ACAT-1 in macrophages is regulated by several cytokines, adipokines, hormones, and bioactive peptides. While Akt involvement in the regulation of cholesterol esterification has not been known, recent studies have shown that the PI3K/Akt/mTORC1 pathway positively regulates multiple genes involved in de novo synthesis of cholesterol and other lipids via transcription factors SREBPs (Duvel et al., 2010; Porstmann et al., 2009). This regulation is

linked to the PI3K/Akt/mTORC1 pathway control of cell growth for which the synthesis of components for a new membrane, such as cholesterol, is required. Interestingly, while ACAT-1 expression in ER contributes to cholesterol homeostasis, the *ACAT-1* gene is not under the control of the SREBP pathway (Goldstein et al., 2006). Our studies suggest that Akt directly and negatively regulates ACAT-1 expression. This parallel stimulation of cholesterol synthesis and suppression of cholesterol esterification in ER may be important for processes requiring the generation of new cell membranes, such as cell growth or phagocytosis.

We have shown that ACAT-1 is polyubiquitinated and degraded in macrophages via the ubiquitin-proteasome system in an Akt3-dependent manner. The mechanism triggering the ubiquitin-proteasome pathway of ACAT-1 degradation needs further investigation. Polyubiquitynation is often induced by protein phosphorylation. Akt directly phosphorylates a number of proteins participating in lipogenesis (Yellaturu et al., 2009). Thus, one possibility is the direct phosphorylation of ACAT-1 by Akt3. This possibility is supported by the following observations: we ruled out three major pathways downstream of Akt (mTOR, GSK-3, and NF-κB) as regulating ACAT-1 expression; there are two potential Akt phosphorylation sites in ACAT-1 (Thr317 and Thr545), and we observed reduced phosphorylation of ACAT-1 using phosphorylated Akt target motif antibody in $Akt3^{-/-}$ macrophages as well as evidence for direct interaction of ACAT-1 and Akt3 in cells. Nevertheless, whether ACAT-1 is directly phosphorylated, or whether another pathway downstream of Akt3 is involved, has yet to be established.

Specific contributions of three Akt isoforms to lipid regulation are not known. We found that CE accumulations were specifically increased in $Akt3^{-/-}$ MPMs. One mechanism providing specificity of Akt function is via regulation of intracellular localization. While intracellular localization of Akt1 and Akt3 could be nuclear, cytoplasmic, or both, depending on the cell type (Santi and Lee, 2010), we observed that in murine and human macrophages, localization of the two isoforms is almost mutually exclusive. Akt1 has nuclear localization with very little staining of the cytoplasm, while Akt3 staining was mostly restricted to the cytoplasm. Localization within the same cellular compartment could facilitate the postranslational regulation of ACAT-1 by Akt3. In agreement with studies by others, we found that ablation of one Akt isoform does not alter the subcellular localization of another Akt isoform (Santi and Lee, 2010). These findings may explain why Akt1 and Akt3 deficiencies have a different effect on lipid accumulation in macrophages, and why Akt3 function is not compensated by Akt1 in these cells. A molecular mechanism behind differential localization of Akt isoforms is still missing. Nevertheless, our finding adds additional evidence that Akt isoforms may have nonredundant functions, even when they are expressed in the same cell.

In conclusion, our study demonstrates that Akt3 plays an antiatherogenic role in vivo, and identifies a previously unknown isoform specific mechanism for this role. Furthermore, the finding of selective regulation of ACAT-1 by Akt3 adds new possibilities for pharmacological regulation of ACAT-1, which may be of interest beyond the field of atherosclerosis.

EXPERIMENTAL PROCEDURES

Animal Procedures

We used littermate-derived, sex-, age-, and genetic background-matched mice in our experiments. $Akt3^{-/-}$ and $Akt1^{-/-}$ mice were generated as previously described (Chen et al., 2005, 2009). $Akt3^{-/-}$ mice were originally created from 129Svj embryonic stem cells (ESCs) and backcrossed ≥6× to C57Bl/6. After the last backcross, heterozygotes were mated to create background-matched WT and $Akt3^{-/-}$ mice for the present studies. $ApoE^{-/-}Akt3^{-/-}$ mice were created from a cross between 6× backcrossed $Akt3^{-/-}$ and $ApoE^{-/-}$ (>20× backcrossed to C57Bl/6) mice to yield double heterozygotes (≥7× backcrossed). These were mated back to the $ApoE^{-/-}$ and screened for $ApoE^{-/-}Akt3^{+/-}$ mice of both genders (≥8× backcrossed). These were then mated to yield background-matched $ApoE^{-/-}$ and $ApoE^{-/-}Akt3^{-/-}$ siblings for the current experiments. Sex- and age-matched 8- to 12-week-old littermates were used for the study. Atherosclerosis was induced by feeding of 8-week-old $ApoE^{-/-}Akt3^{-/-}$ and $ApoE^{-/-}Akt3^{+/+}$ littermates (eight males and four females in each group) with a Western diet containing 0.2% cholesterol and providing 42% calories as fat (TD88137, Harlan Teklad) for 9 weeks. We performed all procedures according to protocols approved by the Cleveland Clinic IACUC.

Bone Marrow Transplantation

Eight-week-old male or female recipient mice were lethally irradiated with a single dose of whole-body irradiation (900 rads) on the day of transplantation. Bone marrow cells from the donor 7-week-old male or female $ApoE^{-/-}Akt3^{-/-}$ and $ApoE^{-/-}Akt3^{+/+}$ mice were isolated and injected into each recipient mouse intravenously. Four weeks later, the mice were fed with a Western diet for 10 weeks and then used for atherosclerotic lesion analysis. Bone marrow and tail tissue of each animal were used to confirm bone marrow reconstitution by PCR analysis.

ACAT-1 and ACAT-2 Immunoprecipitation and Western Blot Analysis

MPMs were cultured with or without 50 μg/ml acLDL for 18 hr. Cells were harvested and lysed. Each sample (100 μg) was incubated overnight at 4°C with rabbit anti-ACAT-1 antibody, rabbit anti-ACAT-2 antibody, or nonimmune rabbit IgG. Then potein A or protein G Sepharose beads were added, and incubation was continued for 4 hr at 4°C. Beads were washed three times with cell lysis buffer, boiled in Laemmli buffer, separated by SDS PAGE, and analyzed by western blotting using mouse anti-ACAT-1, goat anti-ACAT-2, or phospho-Akt substrate antibodies.

In Vitro Akt Kinase Activity Assay

In vitro Akt kinase activity was analyzed using Akt Kinase Assay Kit (Cell Signaling) according to the manufacturer's protocol. Briefly, MPMs were cultured in 10%FBS/RPMI for 24 hr. Cells were harvested, washed once with ice-cold PBS, and lysed with ice-cold nondenaturing lysis buffer. Immobilized phospho-Akt beads were added to cell lysate for immunoprecipitation. The pellet was incubated with 20 μg/ml GSK-3 fusion protein substrate and 0.2 mM ATP in kinase buffer for 30 min at 30°C. Reaction was terminated with 2 × SDS sample buffer. Phosphorylation of GSK-3 was detected by western blotting using phospho-GSK-3 (Ser21/9) antibody.

In Vitro ACAT Activity Assay

Protein samples of $Akt3^{-/-}$ or WT MPMs were incubated with cholesterol, Tyloxapol, BSA, and [^{14}C]-Oleoyl CoA for 15 min at 37°C. Then lipids were extracted, separated, and ^{14}C radioactivity determined by scintillation spectrometry. Full details are given in the Supplemental Information.

Atherosclerotic Lesion Analysis

Mice fed a Western-type diet for 9 or 10 weeks were euthanized by anesthetic overdose. Hearts were perfused with PBS and 4% paraformaldehyde. For en face analysis, the entire aorta from the heart, extending 5–10 mm after bifurcation of the iliac arteries and including the subclavian right and left common carotid arteries, was removed, dissected, stained with oil red O, and evaluated for lesion development by morphometry of scanned images using Adobe Photoshop and NIH Scion Image software (Febbraio et al., 2000).

For the aortic sinus analysis, serial cryosections of 10 μm thickness were taken from the region of the proximal aorta through the aortic sinuses and stained with oil red O, hematoxylin, and light green (Baglione and Smith, 2006). Morphometry of lesions was made using ImagePro software (Media Cybernetics).

siRNA Transfection

Reagents used for siRNA transfection were purchased from Santa Cruz Biotechnology. WT MPMs were treated with control siRNA, Akt1 siRNA, or Akt3 siRNA according to the manufacturer's protocol. The transfection efficiency was assessed using FITC-conjugate control siRNA.

ACAT-1 Protein Stability

MPMs were cultured in RPMI/10% FBS medium in the presence of 10 μg/ml cycloheximide for 0–24 hr and then harvested, and the expression of ACAT-1 and GAPDH was determined by western blotting of total cell lysates.

Statistical Analysis

Data are presented as mean ±SEM. The statistical significance of differences was evaluated using the Student's t test or Mann-Whitney U test. Significance was accepted at the level of $p < 0.05$. When multiple comparisons were made, a Bonferroni correction was made for each test.

SUPPLEMENTAL INFORMATION

Supplemental Information includes six figures, Supplemental Experimental Procedures, and Supplemental References and can be found with this article online at doi:10.1016/j.cmet.2012.04.020.

ACKNOWLEDGMENTS

We thank Dr. Yi Ma for her expert support with flow cytometry analysis. This work was supported in part by National Institutes of Health grants RO1-HL098193 to J.D.S., HL071625 to T.V.B., R01-AG016927 to N.H., and HL077213 and 5P01HL073311-06 to E.A.P.

Received: November 7, 2011
Revised: March 16, 2012
Accepted: April 25, 2012
Published online: May 24, 2012

REFERENCES

Baglione, J., and Smith, J.D. (2006). Quantitative assay for mouse atherosclerosis in the aortic root. Methods Mol. Med. *129*, 83–95.

Chang, T.Y., Li, B.L., Chang, C.C., and Urano, Y. (2009). Acyl-coenzyme A:cholesterol acyltransferases. Am. J. Physiol. Endocrinol. Metab. *297*, E1–E9.

Chen, J., Somanath, P.R., Razorenova, O., Chen, W.S., Hay, N., Bornstein, P., and Byzova, T.V. (2005). Akt1 regulates pathological angiogenesis, vascular maturation and permeability in vivo. Nat. Med. *11*, 1188–1196.

Chen, W.S., Peng, X.D., Wang, Y., Xu, P.Z., Chen, M.L., Luo, Y., Jeon, S.M., Coleman, K., Haschek, W.M., Bass, J., et al. (2009). Leptin deficiency and beta-cell dysfunction underlie type 2 diabetes in compound Akt knockout mice. Mol. Cell. Biol. *29*, 3151–3162.

Das, A., Davis, M.A., Tomoda, H., Omura, S., and Rudel, L.L. (2008). Identification of the interaction site within acyl-CoA:cholesterol acyltransferase 2 for the isoform-specific inhibitor pyripyropene A. J. Biol. Chem. *283*, 10453–10460.

Davies, M.A., Stemke-Hale, K., Tellez, C., Calderone, T.L., Deng, W., Prieto, V.G., Lazar, A.J., Gershenwald, J.E., and Mills, G.B. (2008). A novel AKT3 mutation in melanoma tumours and cell lines. Br. J. Cancer *99*, 1265–1268.

Duvel, K., Yecies, J.L., Menon, S., Raman, P., Lipovsky, A.I., Souza, A.L., Triantafellow, E., Ma, Q., Gorski, R., Cleaver, S., et al. (2010). Activation of a metabolic gene regulatory network downstream of mTOR complex 1. Mol. Cell *39*, 171–183.

Easton, R.M., Cho, H., Roovers, K., Shineman, D.W., Mizrahi, M., Forman, M.S., Lee, V.M., Szabolcs, M., de Jong, R., Oltersdorf, T., et al. (2005). Role for Akt3/protein kinase Bgamma in attainment of normal brain size. Mol. Cell. Biol. *25*, 1869–1878.

Febbraio, M., Podrez, E.A., Smith, J.D., Hajjar, D.P., Hazen, S.L., Hoff, H.F., Sharma, K., and Silverstein, R.L. (2000). Targeted disruption of the class B scavenger receptor CD36 protects against atherosclerotic lesion development in mice. J. Clin. Invest. *105*, 1049–1056.

Fernandez-Hernando, C., Ackah, E., Yu, J., Suarez, Y., Murata, T., Iwakiri, Y., Prendergast, J., Miao, R.Q., Birnbaum, M.J., and Sessa, W.C. (2007). Loss of Akt1 leads to severe atherosclerosis and occlusive coronary artery disease. Cell Metab. *6*, 446–457.

Goldstein, J.L., DeBose-Boyd, R.A., and Brown, M.S. (2006). Protein sensors for membrane sterols. Cell *124*, 35–46.

Han, J., and Nicholson, A.C. (1998). Lipoproteins modulate expression of the macrophage scavenger receptor. Am. J. Pathol. *152*, 1647–1654.

Ikenoya, M., Yoshinaka, Y., Kobayashi, H., Kawamine, K., Shibuya, K., Sato, F., Sawanobori, K., Watanabe, T., and Miyazaki, A. (2007). A selective ACAT-1 inhibitor, K-604, suppresses fatty streak lesions in fat-fed hamsters without affecting plasma cholesterol levels. Atherosclerosis *191*, 290–297.

Kruth, H.S. (2011). Receptor-independent fluid-phase pinocytosis mechanisms for induction of foam cell formation with native low-density lipoprotein particles. Curr. Opin. Lipidol. *22*, 386–393.

Li, A.C., and Glass, C.K. (2002). The macrophage foam cell as a target for therapeutic intervention. Nat. Med. *8*, 1235–1242.

Liang, J.J., Oelkers, P., Guo, C., Chu, P.C., Dixon, J.L., Ginsberg, H.N., and Sturley, S.L. (2004). Overexpression of human diacylglycerol acyltransferase 1, acyl-coa:cholesterol acyltransferase 1, or acyl-CoA:cholesterol acyltransferase 2 stimulates secretion of apolipoprotein B-containing lipoproteins in McA-RH7777 cells. J. Biol. Chem. *279*, 44938–44944.

Manning, B.D., and Cantley, L.C. (2007). AKT/PKB signaling: navigating downstream. Cell *129*, 1261–1274.

Miyazaki, A., Sakashita, N., Lee, O., Takahashi, K., Horiuchi, S., Hakamata, H., Morganelli, P.M., Chang, C.C., and Chang, T.Y. (1998). Expression of ACAT-1 protein in human atherosclerotic lesions and cultured human monocytes-macrophages. Arterioscler. Thromb. Vasc. Biol. *18*, 1568–1574.

Nakatani, K., Thompson, D.A., Barthel, A., Sakaue, H., Liu, W., Weigel, R.J., and Roth, R.A. (1999). Up-regulation of Akt3 in estrogen receptor-deficient breast cancers and androgen-independent prostate cancer lines. J. Biol. Chem. *274*, 21528–21532.

Porstmann, T., Santos, C.R., Lewis, C., Griffiths, B., and Schulze, A. (2009). A new player in the orchestra of cell growth: SREBP activity is regulated by mTORC1 and contributes to the regulation of cell and organ size. Biochem. Soc. Trans. *37*, 278–283.

Rudel, L.L., Lee, R.G., and Cockman, T.L. (2001). Acyl coenzyme A: cholesterol acyltransferase types 1 and 2: structure and function in atherosclerosis. Curr. Opin. Lipidol. *12*, 121–127.

Sano, H., Eguez, L., Teruel, M.N., Fukuda, M., Chuang, T.D., Chavez, J.A., Lienhard, G.E., and McGraw, T.E. (2007). Rab10, a target of the AS160 Rab GAP, is required for insulin-stimulated translocation of GLUT4 to the adipocyte plasma membrane. Cell Metab. *5*, 293–303.

Santi, S.A., and Lee, H. (2010). The Akt isoforms are present at distinct subcellular locations. Am. J. Physiol. Cell Physiol. *298*, C580–C591.

Sekiya, M., Osuga, J., Nagashima, S., Ohshiro, T., Igarashi, M., Okazaki, H., Takahashi, M., Tazoe, F., Wada, T., Ohta, K., et al. (2009). Ablation of neutral cholesterol ester hydrolase 1 accelerates atherosclerosis. Cell Metab. *10*, 219–228.

Stahl, J.M., Sharma, A., Cheung, M., Zimmerman, M., Cheng, J.Q., Bosenberg, M.W., Kester, M., Sandirasegarane, L., and Robertson, G.P. (2004). Deregulated Akt3 activity promotes development of malignant melanoma. Cancer Res. *64*, 7002–7010.

Tabas, I. (2010). Macrophage death and defective inflammation resolution in atherosclerosis. Nat. Rev. Immunol. *10*, 36–46.

Tokuda, S., Mahaffey, C.L., Monks, B., Faulkner, C.R., Birnbaum, M.J., Danzer, S.C., and Frankel, W.N. (2011). A novel Akt3 mutation associated

with enhanced kinase activity and seizure susceptibility in mice. Hum. Mol. Genet. *20*, 988–999.

Tschopp, O., Yang, Z.Z., Brodbeck, D., Dummler, B.A., Hemmings-Mieszczak, M., Watanabe, T., Michaelis, T., Frahm, J., and Hemmings, B.A. (2005). Essential role of protein kinase B gamma (PKB gamma/Akt3) in postnatal brain development but not in glucose homeostasis. Development *132*, 2943–2954.

Worthley, S.G., Helft, G., Corti, R., Worthley, M.I., Chew, D.P., Fayad, Z.A., Zaman, A.G., Fallon, J.T., Fuster, V., and Badimon, J.J. (2007). Statin therapy alone and in combination with an acyl-CoA:cholesterol O-acyltransferase inhibitor on experimental atherosclerosis. Pathophysiol. Haemost. Thromb. *36*, 9–17.

Wright, G.L., Maroulakou, I.G., Eldridge, J., Liby, T.L., Sridharan, V., Tsichlis, P.N., and Muise-Helmericks, R.C. (2008). VEGF stimulation of mitochondrial biogenesis: requirement of AKT3 kinase. FASEB J. *22*, 3264–3275.

Yellaturu, C.R., Deng, X., Cagen, L.M., Wilcox, H.G., Mansbach, C.M., 2nd, Siddiqi, S.A., Park, E.A., Raghow, R., and Elam, M.B. (2009). Insulin enhances post-translational processing of nascent SREBP-1c by promoting its phosphorylation and association with COPII vesicles. J. Biol. Chem. *284*, 7518–7532.

Zhao, B., Song, J., Chow, W.N., St Clair, R.W., Rudel, L.L., and Ghosh, S. (2007). Macrophage-specific transgenic expression of cholesteryl ester hydrolase significantly reduces atherosclerosis and lesion necrosis in Ldlr mice. J. Clin. Invest. *117*, 2983–2992.